Journal of the European Ceramic Society 21 (2001) 2423–2434
www.elsevier.com/locate/jeurceramsoc

In situ growth of elongated α-sialon grains in Li-α-sialon ceramics

Z.B. Yu [a], D.P. Thompson [a,*], A.R. Bhatti [b]

[a] *Materials Division, Department of Mechanical, Materials and Manufacturing Engineering, University of Newcastle upon Tyne, NE1 7RU, UK*
[b] *Structural Materials Centre, DERA Farnborough, GU14 0XL, UK*

Received 2 November 2000; accepted 12 January 2001

Abstract

In situ growth of elongated α-sialon grains has been studied in Li-α-sialon ceramics. The morphology of α-sialon grains is mainly determined by the overall composition, with low m and high n values promoting the anisotropic grain growth of α-sialon needles with even more pronounced effects at higher sintering temperatures and pressures. β-Si_3N_4 starting powder can also facilitate the growth of elongated α-sialon grains since it reduces the number of sites where α-sialon grains can nucleate. The effects of processing parameters on the growth of elongated α-sialon grains were examined. For single-phase α-sialon starting compositions, increases in sintering time do not promote the elongated (or even equiaxed) growth of α-sialon grains after the formation of α-sialon is complete.

Keywords: Anisotropy; Grain growth; Microstructure-final; Sialons; Sintering

1. Introduction

It has been observed and is now well accepted that β-sialon grains normally grow in an elongated manner with a high aspect ratio,[1–3] and this promotes mechanisms such as crack bridging and crack deflection. Thus, β-sialons have a higher strength and fracture toughness, however, α-sialon is generally considered to occur as equiaxed grains and thus its fracture toughness is inferior to that of β-sialon. This limits its applications even though it has an extremely high hardness, much higher than that of β-sialon. According to these observations, extensive work has been focused on the design of two-phase αβ-sialon ceramics which combine the strength and fracture toughness of β-sialon and the hardness of α-sialon to give a tailored combination of mechanical properties. α/β phase ratio can be controlled just by changing the overall composition in Y- and many of the rare earth sialon systems. For example, it has been reported that a composition containing 50% β-sialon and 50% α-sialon showed a hardness (HV_{10}) of ~22GPa and a fracture toughness of 5.5 MPa $m^{1/2}$.[4] This favourable combination of properties has provided α/β-sialon ceramics with many applications, such as in metal cutting tools.[5] Recently the discovery of reversible in situ transformation between α- and β-sialon in some sialon systems is believed to provide another method of tailoring microstructure in αβ-sialon ceramics,[6–9] but this high temperature instability can impose limitations on the use of these ceramics as high temperature structural materials.

More recently, it has been observed that dense α-sialons containing elongated grains can be prepared by carefully selecting the starting composition. Shen et al.[10] found that the morphology of α-sialon grains varies significantly with composition, and elongated grains frequently occurred in the most oxygen rich (i.e. high *n*) compositions in which large amounts of transient liquid had been present. The final samples contained more elongated α-sialon grains and an increased amount of residual glassy grain boundary phase, and therefore, a slight increase in fracture toughness was observed and the hardness was reported to be as high as ~20 GPa. Zhao et al.[11] and Wood et al.[12] also reported that elongated α-sialon grains could form in the Ca-sialon system. However, since the compositions of these samples were located outside the single phase α-sialon region on the α plane, the elongated α grains formed together with other phases, typically long rod-like AlN

* Corresponding author. Tel.: +44-191-2227-202; fax: +44-191-2227-153.
E-mail address: d.p.thompson@ncl.ac.uk, or d.p.thompson@newcastle.ac.uk (D.P. Thompson).

0955-2219/01/$ - see front matter
PII: S0955-2219(01)00197-2

polytypoid grains and large amounts of glassy phase. The sample showed distinct core and rim regions, with slightly different K_{IC} values (4 and 6 $MPam^{1/2}$ respectively), the increase in the latter being attributed to more elongated grains; unfortunately, this limited improvement in K_{IC} was at the expense of a very large decrease in hardness, to only 12–13 GPa, which is because the compositions of the samples are located outside the single phase α-sialon region and contain large amounts of glassy grain boundary phase.

A microstructure based on self-reinforced β-Si_3N_4 elongated crystals can be readily obtained by using α-Si_3N_4 as the starting powder. Chen et al.[13] thought the reverse paradigm of using β-Si_3N_4 as the starting material should hold if self-reinforced α-sialon was to be obtained, and demonstrated that elongated α-sialon grains could be achieved by using high β-Si_3N_4 starting powder and got a fracture toughness comparable to that of β-sialon whilst at the same time keeping the advantage of the high hardness of α-sialon (20–22 GPa). However, it is not totally convincing to attribute the formation of elongated α-sialon grains merely to the use of β-Si_3N_4 starting powder if other observations are taken into account, and β-Si_3N_4 is not as cheap and readily available a starting powder as α-Si_3N_4 powder. Currently, the control and use of anisotropic growth as a route for maximisation of the fracture toughness in sialon ceramics is an active research area.

In this paper, the influence of starting composition and starting powder on texture development in lithium α-sialons is examined, and the effect of processing parameters on the morphology of α-sialon grains is discussed.

Table 1
Compositions used in the general formula $Li_xSi_{12-(m+n)}Al_{(m+n)}O_nN_{16-n}$

Sample	m	n	x
(1.0, 1.0)	1.0	1.0	1.0
(1.0, 1.5)	1.0	1.5	1.0
(1.0, 2.0)	1.0	2.0	1.0
(1.3, 1.2)	1.3	1.2	1.3
(2.0, 1.5)	2.0	1.5	2.0
(2.0, 2.0)	2.0	2.0	2.0

Table 2
Density of bulk samples after sintering for 1 h at different temperatures

Sample	1600°C	1700°C
$(1.0, 1.0)_\alpha$	1.79 (58%TD)	1.88 (61%TD)
$(1.3, 1.2)_\alpha$	1.80 (58%TD)	2.49 (80%TD)
$(2.0, 1.5)_\alpha$	1.80 (58%TD)	2.40 (77%TD)
$(2.0, 2.0)_\alpha$	1.72 (55%TD)	2.21 (71%TD)

2. Experimental procedure

Six compositions were examined in this work. These were located within the single phase α-sialon region on the two-dimensional α-sialon plane.[14] The compositions are listed in Table 1.

Two types of Si_3N_4 powder were used: one was an α rich Si_3N_4 powder (H.C. Starck, Grade B7), containing 90% of α phase; the other was a β rich Si_3N_4 powder (AME), containing 64% of β phase. The subscripts α and β are employed after the (m, n) descriptor to distinguish which starting powder was used. Other starting materials were Al_2O_3, (BDH); AlN (H.C. Starck grade B); Li_2CO_3, (BDH); SiO_2, (BDH). When calculating the composition of the samples, corrections were made for the residual oxygen content of the Si_3N_4 and AlN powders. The powder mix in batches of 30 g was milled in isopropanal for 12 h using sialon milling media in a rubber lined cylinder. The slurry was subsequently dried under an infrared lamp while being stirred. Four grammes of as-mixed powder were initially cold pressed into green-body compacts and then sintered by either pressureless sintering, gas pressure sintering, or hot pressing for 30–90 min at 1600–1800°C under different pressures in a graphite die. Weight loss from samples was measured and bulk densities determined by an upthrust method in Hg. Theoretical density (TD) of single phase products was determined from unit-cell dimensions obtained from Hägg–Guinier X-ray powder photographs and a knowledge of the total molecular weight of the unit-cell; appropriate corrections were made in the case of multi-phase products. Phase analysis of crushed powders was also measured using the Hägg–Guinier XRD camera with

Table 3
Densities and weight losses of bulk samples gas pressure sintered at 1750°C, and then re-sintered at 1800°C

Sample (m, n)*	1750°C, 60 min, 2 atm	WL (%)	1750°C, 60 min, 2 atm/ 1800°C, 60 min, 4 atm	WL (%)
$(1.0, 1.0)_\alpha$	1.86 (60%TD)	−5.3	1.84 (59%TD)	−1
$(1.0,1.0)_\beta$	1.87 (60%TD)	−5.7	1.86 (60%TD)	−0.7
$(1.0, 2.0)_\alpha$	2.48 (80%TD)	−4.1	2.46 (80%TD)	0
$(1.0, 2.0)_\beta$	2.15 (69%TD)	−3.5	2.01 (65%TD)	−5.7
$(2.0, 2.0)_\alpha$	2.51 (81%TD)	−8.4	2.53 (82%TD)	−0.7
$(2.0, 2.0)_\beta$	1.93 (62%TD)	−9.6	1.86 (60%TD)	−6.2

Si as the internal standard, and bulk surfaces polished parallel and perpendicular to the hot pressing direction were examined by Philips diffractometry with Ni filtered CuK_α radiation. Microstructural observations of etched surfaces were carried out on a Hitachi S-2400 and JSM-5300 scanning electron microscopes; polished surfaces were etched by immersion in molten KOH for 10–30 min. All samples were either carbon or gold coated prior to SEM observation to avoid electronic charging.

3. Results and discussion

3.1. Densification of α-sialon ceramics by pressureless and gas pressure sintering

Single phase α-sialon compositions, $(1.0, 1.0)_\alpha$, $(1.3, 1.2)_\alpha$, $(2.0, 1.5)_\alpha$ and $(2.0, 2.0)_\alpha$, were densified by pressureless sintering for 1 h at different temperatures. The results are given in Table 2.

Table 4
Crystalline products and density of samples sintered under different conditions

Sample (m, n)[a]	Sintering condition T (°C), t (min)	Density (g/cm^3)	Crystalline phase	Morphology of alpha phase
$(1.0,1.5)_\alpha$	1700°C, 30	3.00 (95% TD)	α	Equiaxed
$(1.0, 1.5)_\alpha$	1700°C, 90	3.05 (97% TD)	α	Equiaxed
$(1.0, 1.5)_\alpha$/5%U	1730°C, 30	3.12 (99% TD)	α + O′	Equiaxed
$(2.0, 1.5)_\alpha$	1700°C, 30	3.00 (95% TD)	α	Equiaxed
$(2.0, 1.5)_\alpha$	1700°C, 90	3.01 (96% TD)	α + O′ + 21R	Equiaxed
$(2.0, 1.5)_\alpha$/5%U	1730°C, 30	2.94 (93% TD)	α + O′ + 21R	Equiaxed

[a] U: La-U-phase, $La_3Si_3Al_3O_{12}N_2$; O′: β-LiSiON(Al).

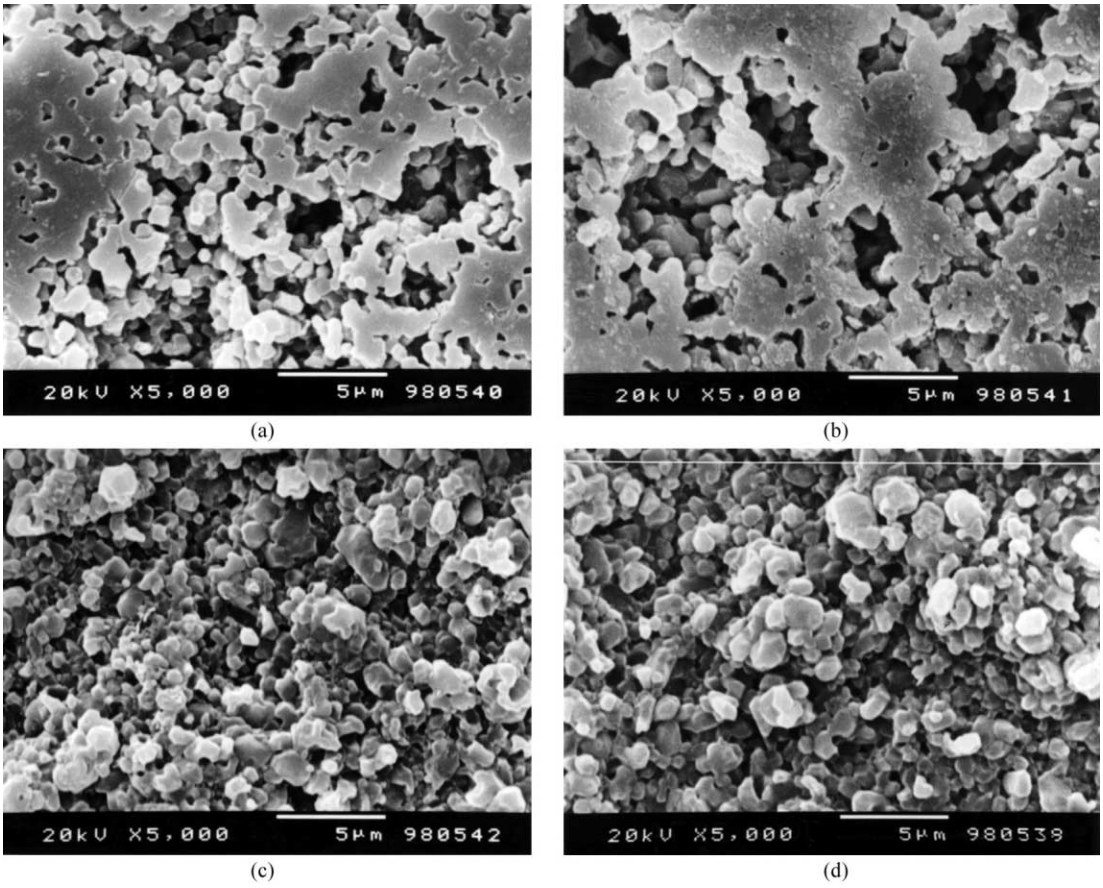

Fig. 1. SEM micrographs of samples $(1.0, 1.5)_\alpha$ and $(2.0, 1.5)_\alpha$ hot-pressed at 1700°C. (a) $(1.0, 1.5)_\alpha$ Sample, 30 min; (b) $(1.0, 1.5)_\alpha$ sample, 90 min; (c) $(2.0, 1.5)_\alpha$ sample, 30 min; (d) $(2.0, 1.5)_\alpha$ sample, 90 min.

As indicated in Table 2, it is very difficult to produce dense α-sialon ceramics even at 1700°C for 1 h by pressureless sintering. Though the samples shrank a little after sintering, the colour was homogeneous throughout and did not change very much. However, earlier studies by Yu and Thompson et al.[14] have shown that nearly all the starting powders react completely to form single phase α-sialon even though the sample may not have fully densified. So, in the next experiment, gas pressure sintering was also tried to see if the densification of single phase α-sialon could be improved under a high nitrogen atmosphere. The samples used had compositions (1.0, 1.0), (1.0, 2.0) and (2.0, 2.0), but both α rich Si_3N_4 and β rich Si_3N_4 powders were used. The sintering results are given in Table 3, from which it can be seen that some weight loss (WL) occurred but this was mainly in the form of CO_2 given off from the starting lithium carbonate. When sintered at 1750°C under 2 atm of N_2 for 1 h, the density of the samples is nearly the same as those of the same compositions sintered by pressureless sintering; furthermore, when these samples were further sintered at 1800°C under 4 atm in N_2 for 1 h, the density did not change very much. It was also noticed that the samples made from β rich Si_3N_4 powder had a lower density compared to those with α rich Si_3N_4 starting powder, suggesting that the densification of the samples containing β rich Si_3N_4 powder is more difficult than those made from α rich Si_3N_4 powder. This is very similar to the formation of β-sialon, from α- or β-rich silicon nitride powders.

From X-ray diffraction results, it was noted that the mixture of starting powders had reacted completely to form α-sialon after 1 h at 1700°C. This is true for both α-rich and β-rich Si_3N_4 powders. However, unlike the formation of β-sialon, for which the transformation from α or β silicon nitride powder to β-sialon has a strong effect on its densification, the transformation from α or β silicon nitride powder to α-sialon makes a very limited contribution to its densification, suggesting that the mechanisms of formation and densification of α- and β-sialon are different. As is well known, the densification of β-sialon is via a "solution-diffusion-precipitation" process, and during sintering, the starting powder, either α- or β-Si_3N_4, is dissolved in the liquid, and as a

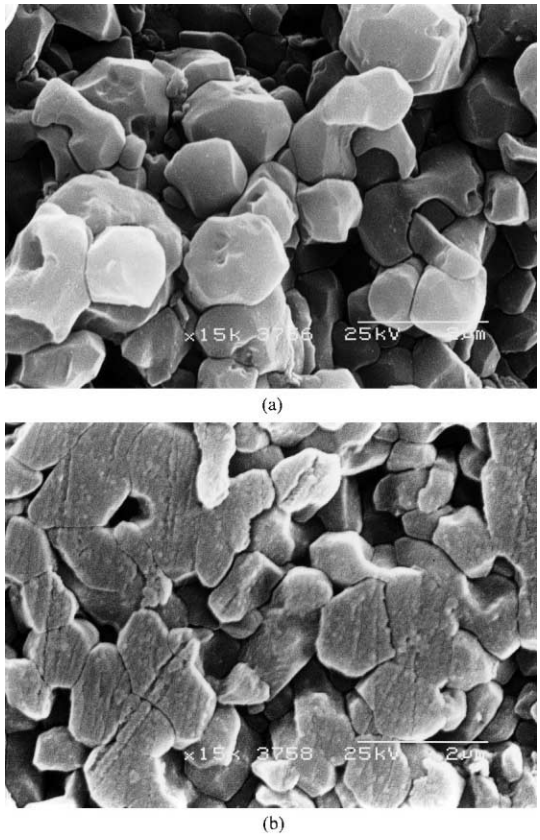

Fig. 2. SEM micrographs of (1.0, 1.0) samples hot-pressed at 1730°C, 30 min, 20 MPa. (a) Made from α-rich Si_3N_4 powder (b) made from β-rich Si_3N_4 powder.

Table 5
Crystalline phase and density of samples sintered under different conditions

Sample	Starting powder	Sintering condition	Density (g/cm^3)	Crystalline phase	Morphology of α′ grain
$(1.0, 1.0)_\alpha$	α	1730°C 30 min 20 MPa	3.02	α′	Equiaxed
$(1.0, 1.0)_\beta$	β	1700°C 60 min 25 MPa	3.03	α′	Equiaxed
$(1.0, 1.0)_\alpha$	α	1730°C 30 min 20 MPa	3.03	α′	Equiaxed
$(1.0, 1.0)_\beta$	β	1700°C 60 min 25 MPa	3.03	α′	Equiaxed
$(1.0, 2.0)_\alpha$	α	1730°C 30 min 20 MPa	3.10	α′	Equiaxed/elongated
$(1.0, 2.0)_\beta$	β	1700°C 60 min 25 MPa	3.09	α′,β(vw)	Equiaxed/elongated
$(1.0, 2.0)_\alpha$	α	1730°C 30 min 20 MPa	3.03	α′	Equiaxed/elongated
$(1.0, 2.0)_\beta$	β	1700°C 60 min 25 MPa	3.07	α′, β(vw)	Equiaxed/elongated
$(1.0, 2.5)_\alpha$	α	1700°C 60 min 25 MPa	3.10	α′	Equiaxed/elongated
$(1.0, 2.5)_\beta$	β	1700°C 60 min 25 MPa	3.10	α′, β, β(w)	Equiaxed/elongated
$(2.0, 2.0)_\alpha$	α	1730°C 30 min 20 MPa	3.00	α′, 21R	Equiaxed/plate
$(2.0, 2.0)_\beta$	β	1700°C 60 min 25 MPa	3.03	α′, 21R	Equiaxed/plate
$(2.0, 2.0)_\alpha$	α	1730°C 30 min 20 MPa	2.97	α′, 21R	Equiaxed/plate
$(2.0, 2.0)_\beta$	β	1700°C 60 min 25 MPa	3.02	α′, 21R	Equiaxed/plate

result of a concentration gradient, diffusion of N and some silicon takes place throughout the liquid phase, followed by nucleation and growth of solid β phase. After the completion of α or β-Si_3N_4 →β phase transformation, the sample is nearly fully dense. When insoluble sintering additives are used, the liquid phase solidifies to a glass after the samples are cooled to room temperature; when soluble sintering additives are used, some species in the liquid (e.g. Al and O) dissolve in the grains resulting in a decrease in the amount of liquid phase at grain boundaries. It has been observed that liquid is always present during the densification of β phase, and in any case, the surplus liquid is necessary to attain full densification of the final β-Si_3N_4 or β-sialon ceramic. However, in the case of the densification of single phase α-sialon ceramics, the densification process is via a 'transient liquid' phase. Thus in compositions designed to form single phase α-sialon, although liquid is formed during the initial sintering stage, as sintering proceeds, this liquid gradually dissolves into α-sialon grains, and once the formation of α-sialon has been completed, most of the original liquid has been accommodated into the α-sialon crystal structure in-situ, as a result of which, the amount of transient liquid is greatly reduced at intermediate stages of densification, and further densification at the final stage becomes very difficult. For this reason, single phase α-sialon starting compositions are hard to densify by pressureless sintering or by gas pressure sintering. Therefore, in order to examine microstructural changes in α-sialon ceramics, in the following experiments, all α-sialon samples were hot-pressed to ensure the formation of a fully dense product.

3.2. Effect of ageing time on α-sialon morphology

Two single-phase α-sialon compositions, $m=1.0$, $n=1.5$ and $m=2.0$, $n=1.5$, i.e. constant n value but different m value, were used to examine the effect of sintering time on microstructure. These two compositions were hot-pressed at 1700–1730°C for 30 and 90 min. under 20 MPa pressure, and the results are given in Table 4.

From Table 4, it can be seen that all the samples densified very satisfactorily at 1700°C under 20 MPa for 30 min. Moreover, further increase in hot-pressing time slightly increased the density suggesting that the densification of the samples is not fully complete after 30 min. X-ray diffraction analysis results showed that the samples consisted mainly of single-phase α-sialon. The fracture surface of samples $(1.0, 1.5)_\alpha$ and $(2.0, 1.5)_\alpha$ were etched by hot molten KOH and examined by SEM, as shown in Fig. 1, which clearly shows the equiaxed morphology of

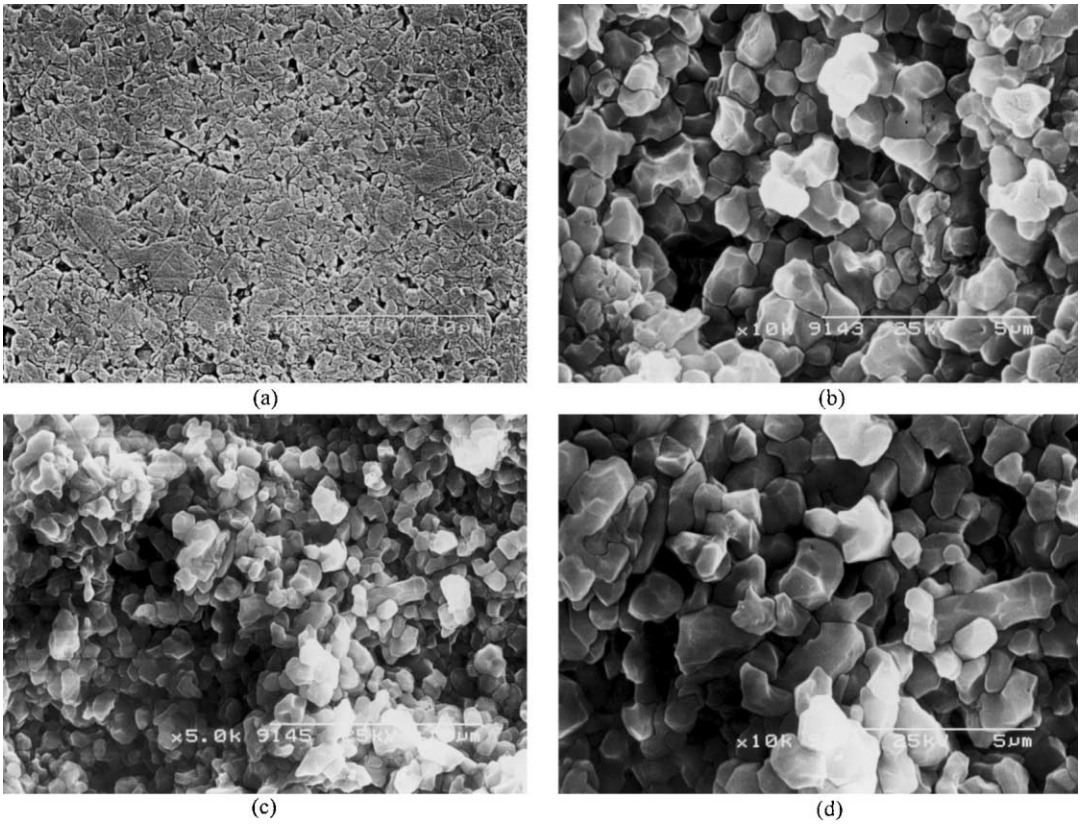

Fig. 3. SEM micrographs of (1.0, 1.0) samples hot-pressed at 1700°C, 60 min, 25 MPa. (a) Low magnification, (b) high magnification (made from α rich Si_3N_4 powder), (c) low magnification, (d) high magnification (made from β-rich Si_3N_4 powder).

the α-sialon grains, indicating isotropic grain growth. It is generally thought that prolongation of the hot-pressing time would result in elongated or enlarged α-sialon grains. For example with prolonged heating at sintering temperature, β-Si_3N_4 or β-sialon grains, which are in equilibrium with the liquid formed during sintering, will grow anisotropically[15] following the empirical grain growth law: $D^n - D_0^n = K_D t$, the rate constant K and growth exponent n being different for the length and the width directions of the β-Si_3N_4 grains. So, during prolonged sintering, the β-Si_3N_4 or sialon grains develop into a rod-like morphology; furthermore, β grain growth in the c direction is observed long after transformation is finished.[16] However, as shown in the microstructures [Fig. 1 (b) and (d)], in single-phase α-sialon compositions, neither elongated nor enlarged α-sialon grains were observed with prolonged sintering and the average size of the grains was very similar to that after hot-pressing for 30 min. [Fig. 1(a) and (c)]. These results indicate that the nucleation and growth rate of α-sialon grains in these two compositions is comparatively fast. But growth stops as soon as the initial starting constituents/transient liquid have disappeared by conversion to α-sialon. An extra 5 wt.% of La-U-phase glass was added to two of

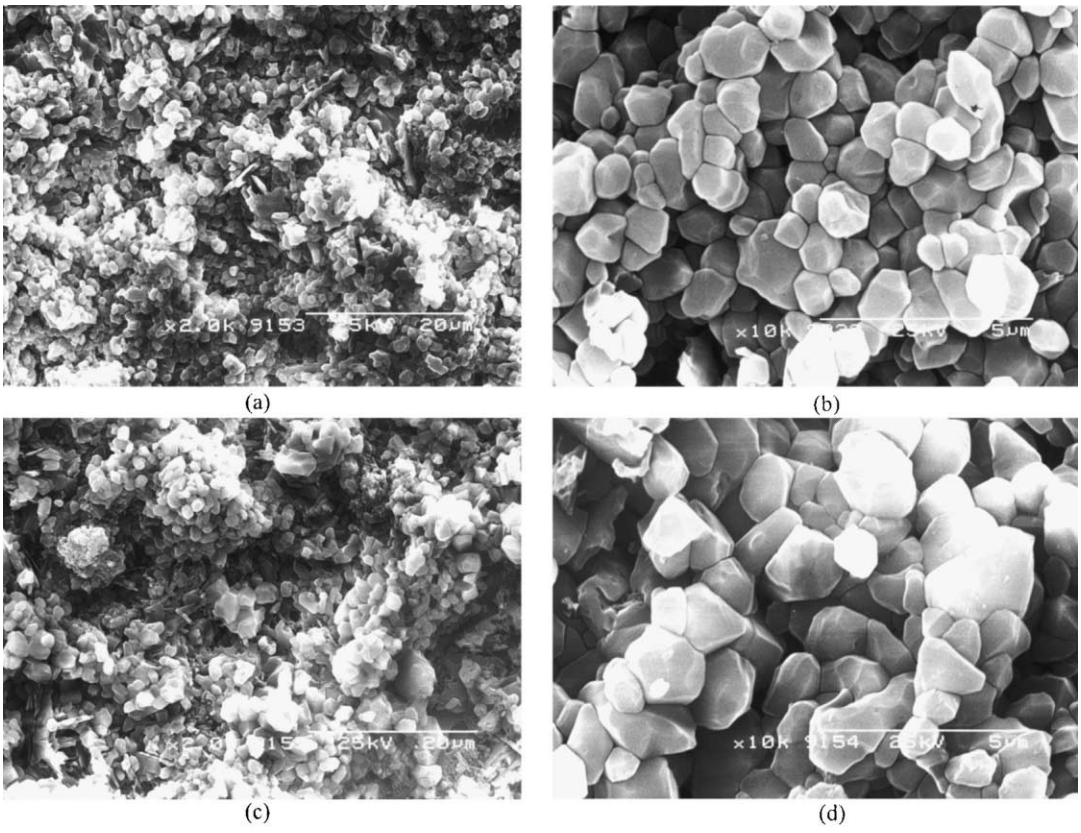

Fig. 4. SEM micrographs of (2.0, 2.0) samples sintered at 1700°C, 60 min, 25 MPa, (a) low magnification (b) high magnification (made from α rich Si_3N_4 powder), (c) low magnification (d) high magnification (made from β-rich Si_3N_4 powder).

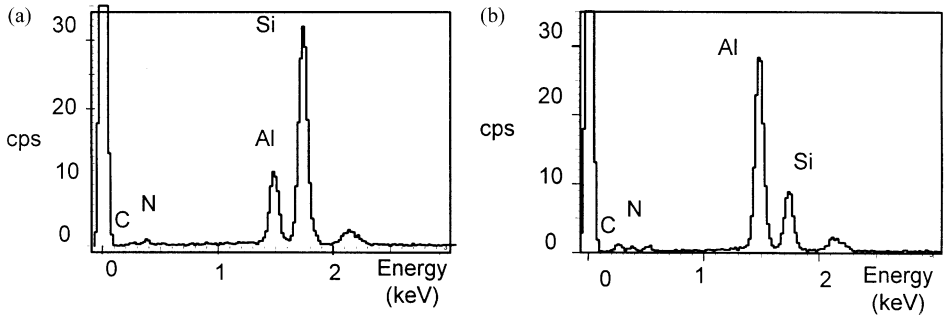

Fig. 5. EDX analysis of α-sialon grain (a) and 21R polytypoid (b) in the (2.0, 2.0) sample.

the compositions to try to create and keep a liquid environment in which α-sialon grains could grow; however, the final microstructure still remained equiaxed except for some plate-like 21R polytypoid grains present.

It is possible that the viscosity of the U-glass phase is still too high at 1730°C to promote an effective diffusion; alternatively, this liquid is not suitable for the growth of Li-α-sialon.

3.3. Effect of chemical composition and starting powder on α-sialon morphology

The above discussion has shown that elongated α-sialon grains cannot grow when the overall composition has an intermediate n value corresponding to compositions located within the single-phase α-sialon region; this is because of the fast nucleation of α-sialon grains. Therefore, in the following experiments, four compositions were chosen for study, the first one having low *m* and *n* values (1.0, 1.0), the second and third having low *m* but higher *n* values (1.0, 2.0) and (1.0, 2.5), and the fourth having both high *m* and *n* values (2.0, 2.0). For these compositions, both α rich and β rich Si_3N_4 powders were used to examine the effect of different starting powders. These compositions were hot-pressed under various conditions and the results are given in Table 5. The table shows that all the samples densified very well by hot-pressing at 1700–1730°C under 20 to 25 MPa for 30–90 min. Both the density and final crystalline phases essentially remained the same regardless of what kind of starting powder was used. However, different starting powders and chemical compositions resulted in different microstructures. The microstructures of both the low and high (*m*, *n*) compositions (1.0,1.0) and (2.0, 2.0) consisted mainly of equiaxed α-sialon grains (Figs. 2 and 3). The polished surfaces of $(1.0, 1.0)_\alpha$ samples are much more difficult to etch than the others. However, it was noticed that the $(1.0, 1.0)_\beta$ sample was relatively easier to etch than the samples made from α rich Si_3N_4 powder (see Fig. 3). These samples were etched under the same conditions (20 minutes in molten KOH), the $(1.0, 1.0)_\alpha$ sample made from α rich Si_3N_4 powder still retaining a well-polished surface [Fig. 3(a)], with only a very thin grain boundary film being etched off and some small holes being caused by fall-out of small grains during ultra-sonic cleaning after etching [shown enlarged in Fig. 3(b)]. However, for the $(1.0, 1.0)_\beta$ sample [Fig. 3(c)], the polished surface had been destroyed by etching and many grains on the polished surface had fallen out during ultra-sonic cleaning. From the higher magnification microstructures Fig. 3(b) and (d), it seems that the average grain size in the $(1.0, 1.0)_\alpha$ sample is slightly smaller than that in the $(1.0, 1.0)_\beta$ sample. Occasionally, some elongated α-sialon grains could be found in holes as shown in Fig. 3 (d). The difference in microstructure caused by the different starting powders might be understood in terms of the different nucleation rate; this idea will be further discussed later.

In the same way, the high *m*, *n* composition (2.0, 2.0) shows a similar tendency [see Fig. 4(a)–(d)], i.e. the average grain size in the $(2.0, 2.0)_\alpha$ sample is smaller than that of $(2.0, 2.0)_\beta$.

For the (2.0, 2.0) samples, the overall composition contains the maximum number of Li and Al atoms which can be incorporated into an Li-α-sialon phase and this α-sialon coexists with very small amounts of 21R polytype phase. Thus small, homogeneous equiaxed α-sialon grains and large plate-like 21R grains are observed. In Fig. 5, the EDX analysis clearly showed the equiaxed grains to be α-sialon and the plate-like grains to be the 21R polytype phase.

Interestingly, more complex microstructures were observed for the (1.0, 2.0) and (1.0, 2.5) samples, these compositions being located within the single phase α-sialon region, but very near to the boundary between single phase α-sialon and the two-phase α/β region. A homogeneous mixture of very fine equiaxed and elongated α-sialon grains, the latter with a high aspect ratio (up to 10), have been observed in samples made either from α rich or β rich Si_3N_4 powder, as shown in Figs. 6 and 7. It is believed that liquid phase plays an important

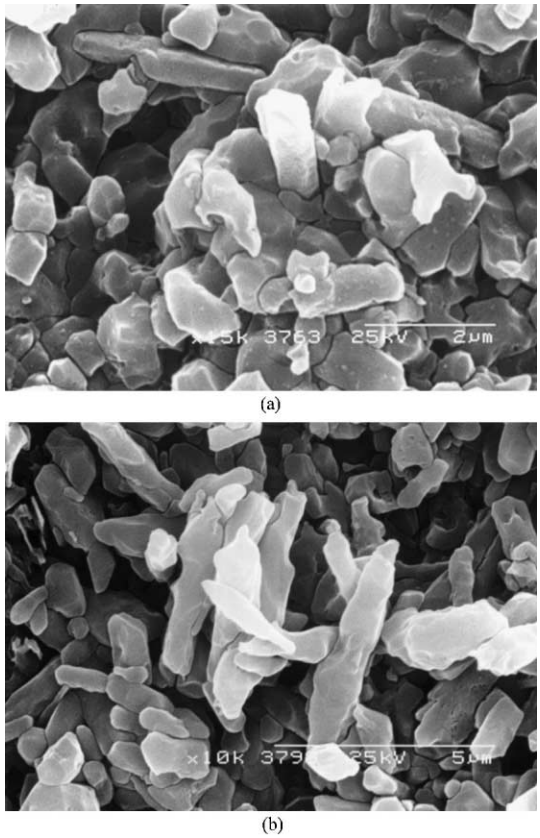

Fig. 6. SEM micrographs of (1.0, 2.0) samples hot-pressed at 1730°C, 30 min, 20 MPa. (a) Sample made from α-rich Si_3N_4 powder, (b) sample made from β-rich Si_3N_4 powder.

role in the formation of elongated α-sialon grains and a previous study reported that an Al-rich liquid with low viscosity could facilitate elongated grain growth in the Ca-α-sialon system.[11] However, in the present study, the (1.0, 2.0) and (1.0, 2.5) samples contained relatively low aluminium and nitrogen but a higher oxygen and silicon content, so, this composition would form a substantial amount of a low-viscosity transient liquid, which would provide a fast pathway for rapid diffusion and give more freedom for nuclei to grow with less impingement upon other grains, thus enhancing the anisotropic grain growth of α-sialon grains along the c-axis.

Although a substantial amount of elongated α-sialon grains are present, all α-sialon grains are actually very fine. The average length of the elongated grains is ~6 μm, and the aspect ratio is about 6 (some exceeding 10). The elongated α-sialon grains are found throughout the sample bulk and surface, but for some reason it seems there are more near the sample surface. XRD analysis indicated that, apart from α-sialon and a very small

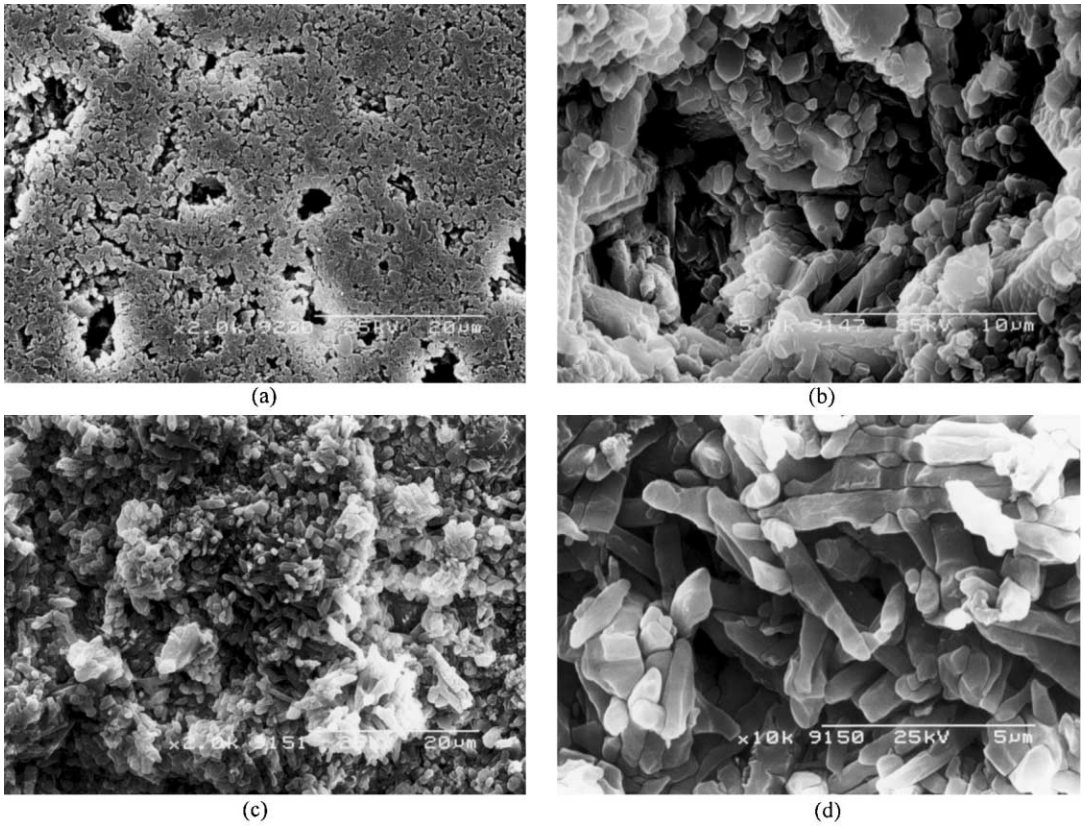

Fig. 7. SEM micrographs of (1.0, 2.0) samples hot-pressed at 1700°C, 60 min, 25 MPa: (a) low magnification, (b) high magnification (made from α rich Si_3N_4 powder), (c) low magnification (d) high magnification (made from β-rich Si_3N_4 powder).

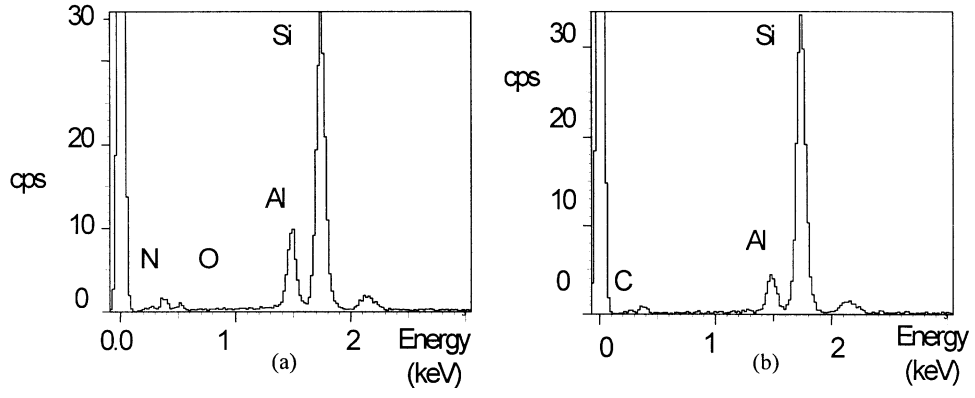

Fig. 8. EDX analysis results for α-sialon grains in the (1.0, 2.0) sample (a) equiaxed α-sialon grains (b) elongated α-sialon grains.

amount of un-reacted very fine β-Si_3N_4 powder in the sample made from β rich Si_3N_4 powder, neither β-sialon nor polytypoid phase was detected as a component phase, eliminating the possibility that the elongated grains were β-sialon or a polytypoid phase. Furthermore, as can be seen from Fig. 8, the EDX analysis results indicated that the elongated and equiaxed grains have a very similar chemical composition which is rich in silicon and not in aluminium, which further eliminates the possibility that the elongated grains are polytype phase as reported in the Ca-sialon system.[12]

In the case of the (1.0, 2.5) samples, the $(1.0, 2.5)_\beta$ sample, which was made from β rich Si_3N_4 powder, consists of α-sialon, β-sialon and un-reacted β-Si_3N_4 powder suggesting that the overall composition is not exactly on the α-sialon plane; its microstructure is given in Fig. 9(e). However, for the $(1.0, 2.5)_\alpha$ sample, which was made from α rich Si_3N_4 powder, it was considered to consist of two regions, namely the 'centre' and the 'edge'. The edge region constitutes the material approximately 2 mm from the edge of the pellet. X-ray diffraction analysis indicated that only α-sialon was present at the centre region of the sample in the form of massive equiaxed and some elongated α-sialon grains [see Fig. 9(a) and (b)]; whereas in the edge region, both α- and β-sialons were detected by XRD, and SEM photos [Fig. 9(c) and (d)] show fine homogeneous equiaxed α-sialon grains and many coarse well-developed β-sialon grains. EDX ana-

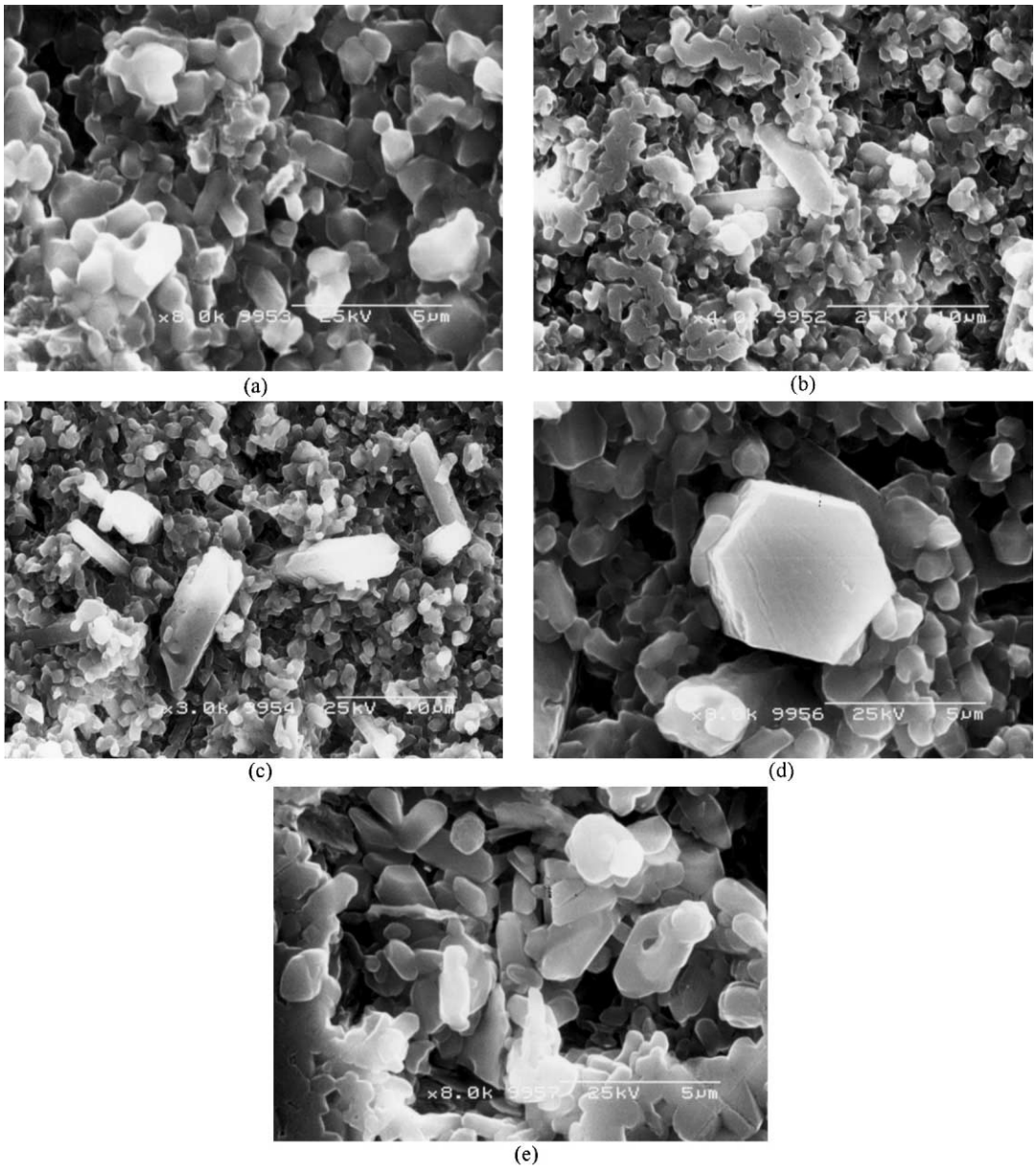

Fig. 9. SEM micrographs of (1.0, 2.5) samples hot-pressed at 1700°C, 60 min, 25 MPa. (a) And (b): the centre region (c) and (d) the edge regions (made from α rich Si_3N_4 powder), (e) the sample made from β-rich Si_3N_4 powder. All pictures were taken under the same magnification: 5k.

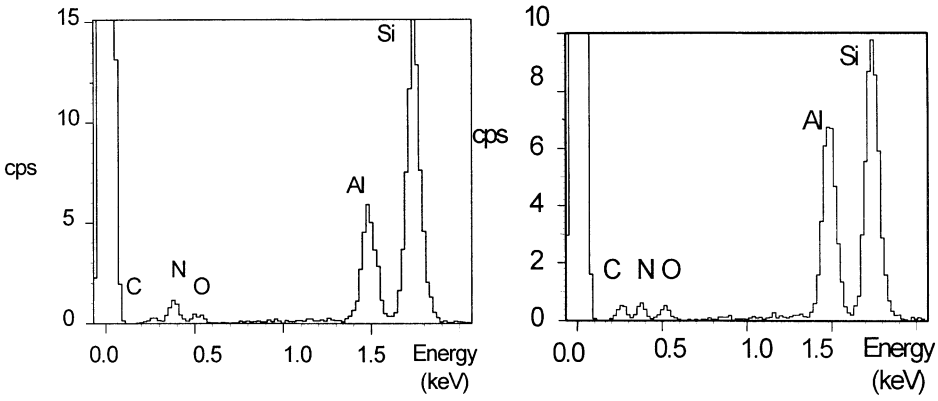

Fig. 10. EDX analysis results of α-sialon grains in sample (1.0, 2.5): (a) equiaxed α-sialon grains; (b) elongated β-sialon grains at the edge of the sample.

lysis indicated that the α-sialon and β-sialon grains had different compositions; it seems that there is more Al in β-sialon than in α-sialon (see Fig. 10).

From the above results, it is believed that it is the overall composition that determines the final microstructure, but that the type of starting powder does have an effect on the morphology of the α-sialon grains. It seems that β rich Si_3N_4 starting powder can facilitate the growth of elongated α-sialon grains, and for instance, there are more elongated α-sialon grains in sample (1.0, 2.0) made from β rich Si_3N_4 starting powder than in that made from α rich Si_3N_4 starting powder. This may be attributed to a different nucleation rate caused by the different starting powders. As the growth of β-sialon grains occurs, the phase transformation from α- or β-Si_3N_4 starting powder to α-sialon during transient liquid phase sintering, can help the anisotropic growth of α-sialon grains. The phase transformation and nucleation rate of α-sialon grains is strongly affected by the starting powder; the nucleation rate of α-sialon from α rich Si_3N_4 starting powder is believed to occur relatively faster than that from β rich Si_3N_4 starting powder because α-Si_3N_4 is more easily dissolved into the liquid than is β-Si_3N_4. Therefore, with an α rich Si_3N_4 starting powder, both the dissolution and diffusion of α-Si_3N_4 in the liquid is rapid which makes the liquid easy to become super-saturated in nitrogen, thus favouring precipitation; in this way reduction in the surface energy becomes the main driving force for densification, as a result of which, substantial amounts of α-sialon nuclei form in the sample, and these subsequently grow and impinge upon one another during hot-pressing, resulting in a microstructure with equiaxed grains. This trend becomes even stronger for those α-sialons with compositions containing very little transient liquid phase during hot-pressing, such as (1.0, 1.0) and (1.0, 1.5) etc. However, with β rich Si_3N_4 starting powder, since it is relatively more difficult to dissolve this into the liquid, the viscosity of the liquid, the rate of nucleation and growth of α-sialons must be low. Therefore, the phase transformation from β-Si_3N_4 to α-sialon cannot be completed during the intermediate stage of densification, and so the densification process is accompanied by grain growth of α-sialon, i.e. the dissolution of small β-Si_3N_4 grains and precipitation of large α-sialon grains. The microstructure of the sample made from β rich Si_3N_4 starting powder is shown in Fig. 7(c) and (d). A characteristic of the microstructure is a bimodal grain size distribution. It consists of a small amount of large, elongated α-sialon grains and a large amount of small equiaxed α-sialon grains. It is believed that the small number of nuclei which formed during phase transformation at the initial stages of densification are responsible for the subsequent abnormal grain growth.

3.4. The orientation of α-sialon grains

In order to examine if there is preferred orientation of α-sialon grains in hot-pressed samples, various specimens were prepared for XRD studies. The crushed powders were examined in a Hägg–Guinier X-ray camera, and the bulk surfaces polished parallel and perpendicular to the hot-pressing direction were examined by a Philips diffractometer with Ni filtered CuK_α radiation. The results are given in Figs. 11 and 12 for the $(1.0, 1.0)_\alpha$ and $(1.0, 2.0)_\alpha$ samples respectively. It was expected that there might be enhanced preferred orientation of α-sialon grains in samples containing elongated grains. However, for the powdered samples, it can be seen from these spectra that there is no obvious change in X-ray peak intensity for planes with different indices, showing that elongated grains if present are lying in different orientations in different grains. In contrast, for bulk samples, a marked difference was observed depending on whether the surface was perpendicular or parallel to the hot-pressing direction. Generally, all (hk0) reflections, i.e. planes parallel to the c-axis, showed a relatively stronger intensity in the surface perpendicular to the hot-pressing direction. This can be seen very clearly from the relative intensity ratio of the (102) and (210)

Fig. 11. X-ray powder diffraction pattern of (a) a powder sample of the composition $(1.0, 1.0)_\alpha$ consisting of equiaxed α-grains and the same sintered sample recorded with the bulk surfaces parallel (b) and perpendicular (c) to the hot-pressing direction.

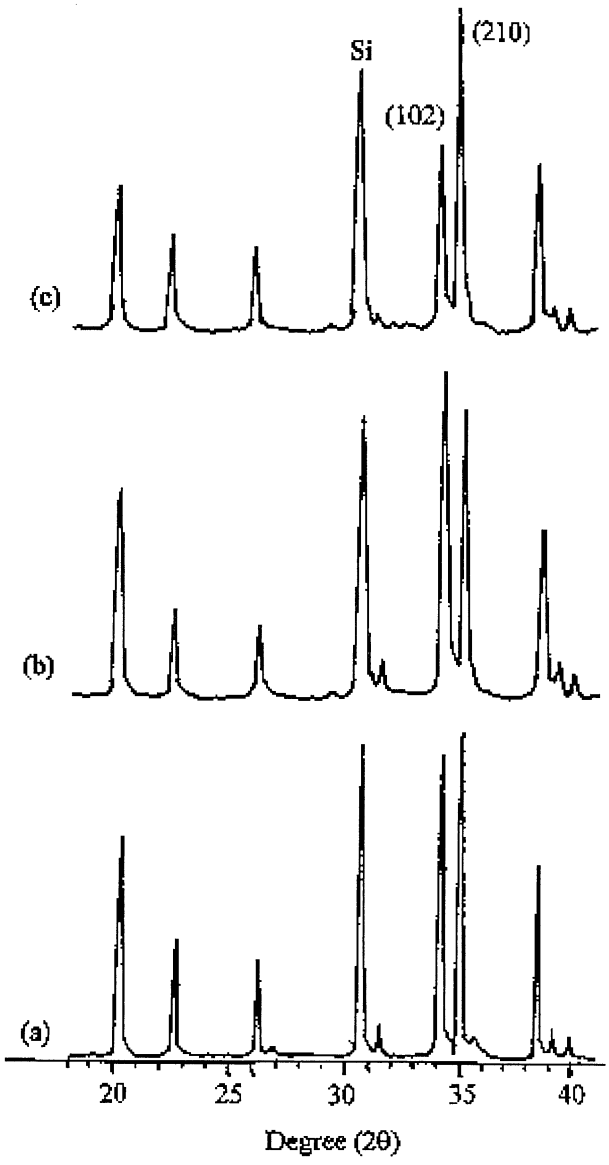

Fig. 12. X-ray powder diffraction pattern of (a) a powder sample of the composition $(1.0, 2.0)_\alpha$ consisting of elongated α-grains and the same sintered sample recorded with the bulk surfaces parallel (b) and perpendicular (c) to the hot-pressing direction.

X-ray diffraction peaks, which changes from~0.6 for the perpendicular section to 1.1 for the parallel section. These results imply that pressure had facilitated grain orientation with the c-axes of α-sialon crystals orienting preferentially normal to the hot-pressing direction. Similar effects have been reported in other cation stablised α-sialons, such as Ca-[11, 12, 17] and rare earth[10, 13] α-sialon systems. However, the intensity of the (210) peak is always higher than the (102) peak if the sample is oriented perpendicular to the pressing direction regardless of the presence of elongated grains. Thus Fig. 11 [sample (1.0, 1.0) containing no elongated grains] shows the same orientation effect as Fig. 12 [sample (1.0, 2.0) containing a large amount of elongated grains], indicating that all α grains are orientated regardless of size, XRD is, therefore, not a useful technique for identifying the presence of elongated α grains.

4. Conclusions

(1) The densification of α-sialon ceramics occurs via transient liquid phase sintering. Dense single phase Li-α-sialon ceramics can only be achieved using high sintering temperatures (1700–1750°C) and pressures (20–25 MPa).

(2) The morphology of α-sialon grains is mainly determined by the overall composition. Low *m* and high

n value compositions can promote anisotropic grain growth of α-sialon because of the large volume of low viscosity transient liquid formed during sintering. β-Si_3N_4 starting powder can facilitate the growth of elongated α-sialon grains since it can result in a relatively low nucleation rate of α-sialon. Processing parameters also have a strong effect. An increase in sintering time cannot promote the growth of α-sialon grains after the formation of α-sialon is complete because most of the liquid has been accommodated in the α-sialon structure. High sintering temperatures and high pressures favour the formation of elongated α-sialon grains. More transient liquid can be formed at high temperatures and a preferred orientation of the α-sialon grains is promoted by high pressures, which accelerates the growth of α-sialon grains in a particular direction.

Acknowledgements

The authors would like to thank the Defence Evaluation and Research Agency (DERA) for financial support.

References

1. Lange, F. F., Relation between strength, fracture energy, and microstructure of hot-pressed Si_3N_4. *J. Am. Ceram. Soc.*, 1973, **56**, 518–522.
2. Wötting, G., Kanka, B. and Ziegler, G., Microstructural development, microstructure characterisation and relation to mechanical properties of dense silicon nitride. In *Non-oxide Technical and Engineering Ceramics*, ed. S. Hampshire. Elsevier, London and New York, 1986, Chapter 29, pp. 83–96.
3. Tani, E., Umebayashi, S., Kishi, K., Kobayashi, K. and Nishihima, M., Effect of size of grains with fibre-like structure of Si_3N_4 on fracture toughness. *J. Mater. Sci. Lett.*, 1454, **4**, 1985.
4. Ekström, T., α-Sialon and αβ sialon composites: recent research. In *Engineering Ceramics'96: Higher Reliability through Processing*. Kluwer Academic Publishers, The Netherlands. 1997, pp. 147–167.
5. Ekström, T., Effect of composition, phase content and microstructure on the performance of yttrium SiAlON ceramics. *Mater. Sci. Eng.*, 1989, **A109**, 341–349.
6. Mandal, H., Thompson, D. P. and Ekström, T., Reversible α↔β sialon transformation in heat-treated sialon ceramics. *J. Eur. Ceram. Soc.*, 1993, **12**, 421–429.
7. Thompson, D.P., α = β Sialon transformation. In *Tailoring of Mechanical Properties of Si_3N_4 Ceramics*, ed. M. J. Hoffman and G. Petzow. Kluwer Academic Publishers. The Netherlands, 1994, 125–136.
8. Yu, Z. B., Thompson, D. P. and Bhatti, A. R., Transformation and thermal stability of Li-α-sialon ceramics. *J. Eur. Ceram. Soc.*, 2000, **20**, 1815–1828.
9. Yu, Z. B., Thompson, D. P. and Bhatti, A. R., Reverse α⟺β phase transformation in Li-α-sialon ceramics. In *International Symposium on Nitrides II*, Trans Tech Publications, Zurich, Switzerland. 9–11 June, University of Limerick, Ireland, 1998, pp. 264–268.
10. Shen, Z. J. et al., α Sialon grains with high aspect ratio-utopia or reality. In *Engineering Ceramics'96: Higher Reliability through Processing*, ed. G. N. Babini et al. Kluwer Academic Publishers, The Netherlands, 1997, pp. 169–178.
11. Zhao, H., Swenser, S. P. and Cheng, Y.-B., Elongated α-sialon grains in pressureless sintered sialon ceramics. *J. Eur. Ceram. Soc.*, 1997, **18**, 1053–1057.
12. Wood, C. A., Zhao, H. and Cheng, Y.-B., Microstructural development of Ca-α-sialon ceramics. *J. Am. Ceram. Soc.*, 1999, **82**(2), 421–428.
13. Chen, I. W. and Rosenflanz, A., A tough SiAlON ceramic based on alpha-Si_3N_4 with a whisker-like microstructure. *Nature*, 1997, **389**, 701–704.
14. Yu, Z. B., Thompson, D. P. and Bhatti, A. R., Preparation and single phase region of Li-α-sialon ceramics. *Brit. Ceram. Trans.*, 1998, **97**(2), 41–46.
15. Lai, K. R. and Tien, T. Y., Kinetics of beta silicon nitride grain growth in silicon nitride ceramics sintered under high-nitrogen pressure. *J. Am. Ceram. Soc.*, 1993, **76**(1), 91–96.
16. Carroll, D. F. and Pyzik, A. J., *44th Pac. Coast Reg. Meet.* Am. Ceram. Soc, San Diego, 1991.
17. Wang, H., Cheng, Y.-B., Muddle, B. C., Gao, L. and Yen, T. S., Preferred orientation in hot-pressed Ca α-sialon ceramics. *J. Mater. Sci. Lett.*, 1996, **15**, 1447–1449.